Wang, J., Sadowski, A.J. & Camara, A. (2019) The effect of the rupture distance of the earthquake on the seismic response of wind turbine support towers. *Proceedings of the 7th International Conference on Structural Engineering, Mechanics and Computation*. Accepted Manuscript.

The effect of the rupture distance of the earthquake on the seismic response of wind turbine support towers

J. Wang
Department of Architecture and Civil Engineering, University of Bath, Bath, UK
A. J. Sadowski
Department of Civil and Environmental Engineering, Imperial College London, London, UK
A. Camara
School of Mathematics, Computer Science and Engineering, City, University of London, London, UK

ABSTRACT: The global growth in wind energy suggests that wind farms will increasingly be deployed in seismically active regions, with large arrays of similarly designed structures potentially at risk of simultaneous failure under a major earthquake. The distance between the wind farm and the epicentre of the earthquake affects the frequency content of the seismic action and this may in turn have a significant impact on the performance of the wind turbines. This study presents the seismic analysis of a wind turbine subject to a large number of seismic records corresponding to events with different rupture distances, and the nonlinear dynamic analysis of a detailed finite element model of the structure with realistic imperfections. The geometrically and materially nonlinear dynamic analyses conducted demonstrate that apart from the typical long-period vibration modes there are higher-order frequencies of the structure that can have a significant contribution in the response, and the importance of these is affected by the epicentral distance of the earthquake and by the imperfections of the tower.

1 INTRODUCTION

It is recognised that future energy needs must draw on renewable sources to reduce CO_2 emissions. Wind energy is currently representing the fastest growth area of all renewables. For this reason an increasing number of wind farms are constructed in earthquake-prone regions, with the risk of simultaneous failure of entire arrays of similarly designed structures in these farms under the action of strong ground motions.

Relatively few published works focused on the seismic response of the wind turbine towers. Nuta *et al*. (2011) performed an incremental dynamic analysis (IDA) in an 80-m tall 1.65-MW wind turbine steel tower and observed that it performed well under seismic actions due to its long fundamental period. However, they also observed that collapse can occur suddenly if the elastic limit is exceeded during the earthquake. This was also concluded by Zhao *et al*. (2019), who also noticed that under far-field earthquake excitations the bottom region of the tower is critical in most cases, but in some records corresponding to rock grounds that were dominated by low vibration periods the upper part of the tower triggers the collapse. This is because the contribution of high-order vibration modes in those earthquakes reduces the time that it takes for the structure to collapse, as well as the energy that it can dissipate before this happens. It was verified that the higher the position of the plastic hinge in the tower the more brittle the failure is.

The previous works consider that the towers are near-cylindrical and perfect tubular structures. Sadowski et al. (2017) considered for the first time the welding imperfections in the tower in the nonlinear seismic analysis of the structure. They observed that these imperfections have almost no influence in the elastic seismic response but they affect significantly the intensities of the ground accelerations at which damage initiates, as well as on the failure location. This study also compared the response under two groups of 10 far-field and near-field earthquakes to conclude that the response can be more damaging under near-field earthquakes with pulse-like effects and large vertical accelerations.

These results, along with the recent literature review on the topic presented by Katsanos *et al*. (2016), suggest the need for comprehensive studies of the influence of the distance between the epicenter of the earthquake and the structure (referred to as rupture distance in the following, R_{epi}). This is the scope of the present study which is divided in two main segments: (a) the study of the linear elastic seismic response of a wind turbine under a large number of records (more than 2,500), and (b) the nonlinear time-history seismic analysis of selected records with different rupture distances, with and without imperfections. The results show the importance of these aspects.

2 DESCRIPTION OF THE STRUCTURE

The structure considered in this study is a 61-m hollow tubular steel tower supporting a 1.5-MW capacity. It was designed to resist a reference wind speed of 42.5 m/s at the hub but without explicit consideration of the seismic response. The outer diameter of the tapering tower varied from 4035 mm at the base to 2955 mm at the top, whilst the wall thickness ranges from 25 mm at the base to a minimum of 10mm near the top. Consequently, the diameter-to-thickness ratios vary from ~161 at the base to a maximum of ~375 in the upper regions of the tower (Fig. 1(a). The material of the tower is S355 steel. The mass of the support tower was approximately 91 tonnes. Full details of the tower geometry are given in Sadowski *et al*. (2017).

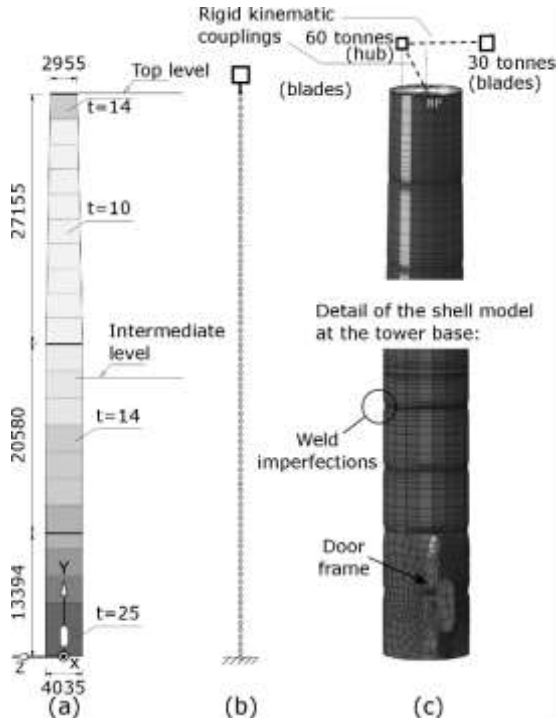

Figure 1. (a) Geometry of the tower, the shading denotes the thickness (darker means thicker), the horizontal lines represent welding between segments. (b) Beam element model. (c) Shell model with imperfections (exaggerated for illustration). Units in mm.

The finite element models of the structure with beam and with shell elements developed in ABAQUS (2017) that are shown in Fig. 1 (described in the following sections) gave a fundamental vibration mode of the tower of T_1 = 2.09 s. This result is very close to the value measured experimentally in this structure (Dai *et al*., 2015). None of the numerical models consider soil-structure interaction, and the base of the towers is completely fixed. This was proved admissible when capturing the dominant vibration modes of the structure.

3 SEISMIC ACTION

A total of 2660 three-directional earthquake records extracted from the PEER-NGA (Ancheta *et al*., 2013) database have been considered in this study. The only conditions imposed in the selection of these records is that the moment magnitude (M_W) is above = 5 and the epicentral distance is below R_{epi} = 300 km. The spectral shape of the records is intentionally not specified in the selection of the records in order to explore its influence in the seismic response of the tower. The two uncorrelated horizontal components of the records are applied in the X and Z directions (Fig. 1(a)). The vertical component is applied in the Y direction.

The definition of the Intensity Measures (IMs) is important in the seismic analysis of structures and it is discussed in this study on wind turbine towers. Both structure-independent and –dependent IMs have been used. The structure-independent IMs are modular versions of the traditional Peak Ground Acceleration (PGA), Velocity (PGV) and Displacement (PGD) combining the two horizontal components of the records:

$$\overline{\mathrm{PGA}} = \sqrt{\left[\max_t\left(\ddot{u}_{g,X}(t)\right)\right]^2 + \left[\max_t\left(\ddot{u}_{g,Z}(t)\right)\right]^2} \quad (1)$$

$$\overline{\mathrm{PGV}} = \sqrt{\left[\max_t\left(\dot{u}_{g,X}(t)\right)\right]^2 + \left[\max_t\left(\dot{u}_{g,Z}(t)\right)\right]^2} \quad (2)$$

$$\overline{\mathrm{PGD}} = \sqrt{\left[\max_t\left(u_{g,X}(t)\right)\right]^2 + \left[\max_t\left(u_{g,Z}(t)\right)\right]^2} \quad (3)$$

where $u_{g,i}$ is the ground displacement in the horizontal direction "*i*" (with $i = X, Z$). The overdot in $u_{g,i}$ represents the time-derivative. The structure-dependent IM is the modular spectral acceleration at the fundamental period of the tower:

$$\overline{S_a}(T_1) = \sqrt{\left[S_{a,X}(T_1)\right]^2 + \left[S_{a,Z}(T_1)\right]^2} \quad (4)$$

where $S_{a,i}$ is the spectral acceleration of the ground motion in the horizontal direction "*i*" (with $i = X, Z$) evaluated at T_1 = 2.09 s. This mode is considered to be the same in any horizontal direction because the relative position between the door and the hub/blade system, which are the only sources of asymmetry in the tower, have a negligible effect (Dai *et al*., 2017).

4 LINEAR ELASTIC SEISMIC ANALYSIS

4.1 *Numerical model*

An extensive linear elastic seismic analysis considering the 2660 records of the proposed set of earthquakes is conducted first. A preliminary analysis has shown that in the elastic range the model of the tower with beam elements offers the same accuracy as a

more detailed model with shell elements that include the door opening, stiffeners and weld depression imperfections. For this reason the study started with a simple three-dimensional model with beam elements that represent the variation of the circular section along the height. The elements have a typical length of 270 mm (~ 0.44% of the tower height) and linear variation of the curvature within the element. The mass of the hub and the blades is represented with lumped masses as shown in Fig. 1(b). The advantage of the beam model is its computational efficiency, something essential due to the extremely large number of analysis conducted in this work. For this reason, only the peak elastic seismic response is studied by means of the Modal Response Spectrum Analysis (MRSA). The three-directional response spectra of all the records was obtained for this study with a damping ratio of 1% to represent the 'parked' condition of the turbine blades in all wind directions or operational conditions with side-to-side wind directions. This is considered the critical scenario for the seismic response of the tower because lower damping is associated with larger seismic demands. The modal responses are superimposed through the Complete Quadratic Combination and the directional combination follows the Square Root of the Sum of Squares (SRSS) rule. The peak response is presented in terms of the peak horizontal displacement ($\bar{u}$) and the peak bending moment ($\overline{M}$). These are modular responses that result from the square root of the sum of the squares of the corresponding displacements or bending moments in the two horizontal directions (X and Z).

Fig. 2 shows the peak displacement at the top level in terms of the epicentral distance of the earthquakes. No clear trend is observed because the original records have very different intensities, which suggests the need for scaling with respect to an appropriate IM.

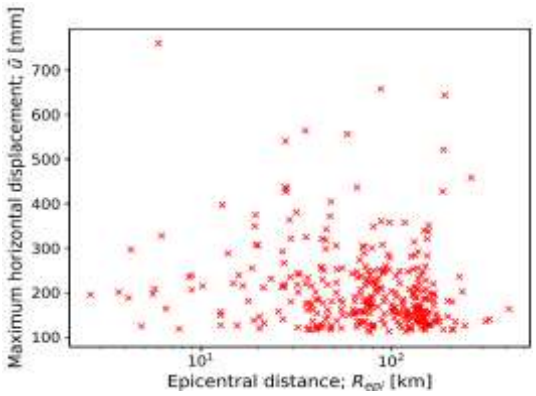

Figure 2. Peak horizontal displacement at the tower top versus the epicentral distance. MRSA with unscaled records.

Fig. 3 presents peak displacement at the Top level of the tower (Fig. 1(a)) for all the earthquakes in terms of their IMs. It is clear that the structure-independent IMs, particularly the PGA and the PGD, are not good representatives of the structural behaviour. This is attributed to the uncorrelation between the spectral response for a zero-value vibration period and that at the dominant mode of the structure: $S_a(T_1)$. The latter governs the response in structures dominated by the fundamental mode like this cantilever tower with a large mass at its top, and for this reason there is an almost linear trend between $S_a(T_1)$ and the displacement at the top. It can be concluded that, as expected, $S_a(T_1)$ is a very efficient IM for the seismic analysis of wind turbine towers: regardless of the spectral shape of the record (characterized by the epicentral distance or the moment magnitude, among others), the value of $S_a(T_1)$ dominates the seismic displacements of the structure. In the following, only $S_a(T_1)$ will be discussed as the IM.

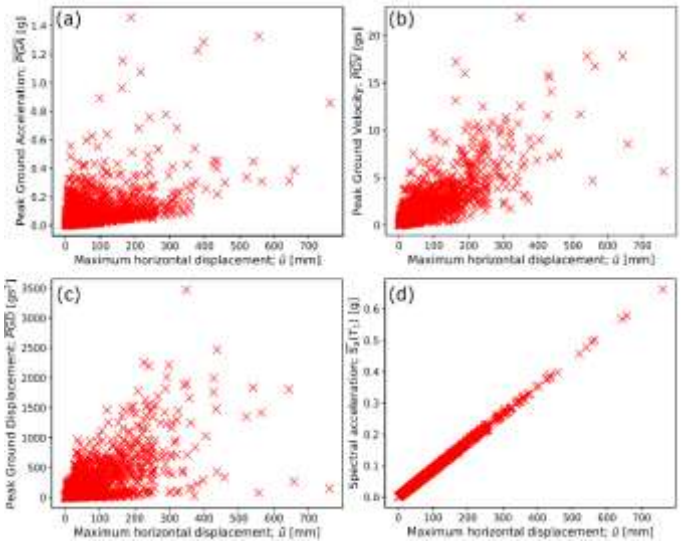

Figure 3. Peak horizontal displacement at the tower top versus different IM: (a) PGA, (b) PGV, (c) PGA, (d) Spectral acceleration at the fundamental period. MRSA with unscaled records.

The previous results show the large variability of $S_a(T_1)$ in the selected set of records (from less than 0.01 g to more than 0.65g in Fig. 3(d)) and the need for scaling to study the influence of the epicentral distance. Fig. 4 presents the peak response of the structure after scaling the records so that their modular $S_a(T_1)$ is 0.5g. The earthquakes with unscaled $S_a(T_1)$ below 0.1g were removed from the plot to avoid unrealistic scaling factors. The responses in terms of displacements and bending moments are clearly organised close to the horizontal lines that represent the arithmetic averages of the results. This is particularly clear in Fig. 4(a) in terms of the displacements at the top and at the intermediate sections of the tower (indicated in Fig. 1(a)), which indicates that the value of $S_a(T_1)$ is more important than the epicentral distance. Nevertheless it is observed that in the range of far-field earthquakes with R_{epi} between 20 and 120 km there is a larger influence of the rupture distance in terms of the peak displacements. The influence of R_{epi} in the bending moments is illustrated in Fig. 4(b). The bending moments depend on the second derivative of

the displacements and they are more sensitive to the contribution of higher-order vibration modes. This gives more importance to the spectral shape below the fundamental period and it explains why for the same IM some records give much higher bending moments at the intermediate section and, especially, at the base. This is particularly significant for near-field earthquakes with R_{epi} below 10 km.

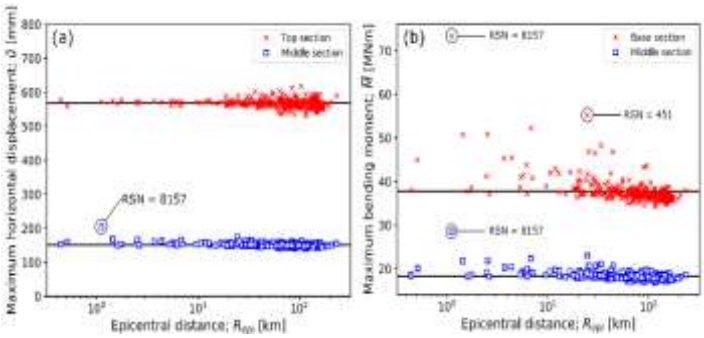

Figure 4. Influence of the epicentral distance on the peak elastic seismic response: (a) displacements, (b) bending moments. MRSA with records scaled to $S_a(T_1)$ = 0.5g.

Fig. 4 allows to identify the Record Sequence Number (RSN) of critical earthquakes with R_{epi} in different ranges in which the response of the tower is particularly large. These are summarised in Table 1 and they are considered in the nonlinear study. Both records were recorded in similar grounds and have similar significant durations (approximately 30 s).

Table 1. Selected earthquakes.

RSN	Name (year)	R_{epi} [km]	M_W	$v_{s,30}$ [m/s]	$S_a(T_1)$ [g]
8157	Christchurch (2011)	1.11	6.2	422	0.16
451	Morgan Hill (1984)	24.55	6.2	561.4	0.14

5 INELASTIC SEISMIC ANALYSIS

5.1 *Numerical model*

The goal of the nonlinear seismic analysis is to study the energy dissipation and the influence of geometric imperfections such as weld depressions in the tower wall for the two records presented in Table 1. The wall was modelled using a mesh of linear reduced-integration finite-strain S4R general purpose shell elements. The steel model follows an ideal elastic–plastic material law that was applied with a yield stress of 355 MPa, a Poisson's ratio of 0.3, an elastic modulus of 200 GPa and a density of 7850 kg/m^3. In order to improve the accuracy of the response in the advance loading stages, simple 'frictionless' tangential and 'hard' normal self-contact was permitted in the tower. The internal flanges at different locations of the tower were modelled as an artificially thick shell segment. The door opening was modelled as an elliptical cut-out including a metallic stiffener around its perimeter defined with beam elements. The construction of the tower is based on the welding of the different segments shown in Fig. 1(a). As a result of shrinking during post-weld cooling an inward curl appears and it may affect significantly the seismic response of the structure (Sadowski *et al.*, 2017). In this work, two types of towers have been considered in terms of their axisymmetric weld imperfections, defined through the Fabrication Tolerance Quality (FTQ): FTQ '0' (no imperfections, 'perfect' quality) and FTQ 'C' (approximately 22.5-mm depressions for the tower geometry considered herein, 'normal' quality). More details about the shell model and the imperfections are given in Sadowski *et al.* (2017).

In each step of the nonlinear response history analysis (NLRHA) the coupled system of dynamics is solved using the HHT implicit algorithm with automatic time-stepping (ABAQUS, 2017). The structural damping is defined by a Rayleigh distribution with 1% damping at the lowest and the highest vibration modes of interest (2.09s and 0.044s, respectively).

The three components of the earthquakes are scaled progressively to explore the linear and the nonlinear responses of the tower up to collapse following using the Incremental Dynamic Analysis (IDA) framework. Each value of the IM is then plotted against the response represented by an Engineering Demand Parameter (EDP). In this work, the EDP is chosen as the dissipated plastic energy in the entire tower at the end of the earthquake (E_P), which is zero when the response is completely elastic. This EDP is preferred to the more conventional displacement at a reference point because it is not clear where a hinge location is in advance, therefore it is difficult to make sense of the lateral drift at the top.

5.2 *Nonlinear time-history analysis results*

Fig. 5 shows the results of the IDA conducted in the tower under the two records and for different imperfection levels. The original near-field earthquake, without scaling factors, is able to produce a slight damage in the tower with $S_a(T_1)$ = 0.16 g. This damage is concentrated at the weld between the upper segments of the structure, as it is described in Fig. 6. However, the original far-field excitation is not able to damage the tower, not even after scaling to $S_a(T_1)$ = 0.16 g. In fact, the IM of the far-field earthquake that starts the damage in the tower is 0.28 g and 0.42 g for the model with and without imperfections, respectively, i.e. 1.7 and 2.6 times larger $S_a(T_1)$ than the corresponding value in the near-field record. The effect of the imperfections is significant but the way in which it affects the seismic behaviour of the tower depends strongly on the particular record considered and its intensity. In the far-field earthquake the imperfections reduce by 66.7% the value of the $S_a(T_1)$ above which damage starts but tower is considered to

collapse (due to lack of convergence of the analysis) at the same IM. In the near-field earthquake the effect of the imperfections is almost opposite. They have no influence on the IM that marks the onset of damage, although Fig 6 indicates that it is more distributed when there are weld depressions. However, the imperfections seem to help the structure to resist 25% stronger seismic actions at the collapse level, which in the case of the structure with imperfections occurs due to the development of a full plastic hinge at the top third of the tower. Further NLRHA on a larger number of records need to be conducted to explore in detail the important effect of the imperfections.

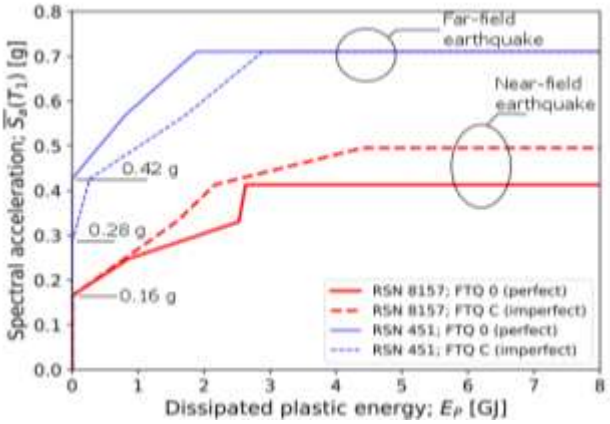

Figure 5. Spectral acceleration versus energy dissipated by plasticity in the tower. NLRHA.

Figs. 6 and 7 compare the deformation along the tower at the end of the two earthquakes or at the collapse stage. It is clear that the failure mechanism is due to the concentration of damage at one of the connections between the segments of the towers, even in the structure without imperfections. This is due to the change of thickness between these segments. After the full hinge is developed a mechanism is formed in the region above, with the large mass of the hub and the blades (90 tonnes) introducing significant p-Δ effects at the hinge and accelerating the collapse. The weld depressions seem to distribute the damage at different segment connections for lower IMs but for larger values the damage is concentrated at a single section and collapse usually occurs faster than in the perfect structure. The difference between the response under near-field and far-field earthquakes is normally in the position of the damaged section. In the near-field earthquake the hinge is developed at the upper third of the tower, where the section has smaller diameter and thickness, which has less capacity to dissipate energy by plasticity than in lower sections. This is due to the larger contribution of high-order modes in near-field earthquakes, which excite more the top region of the tower.

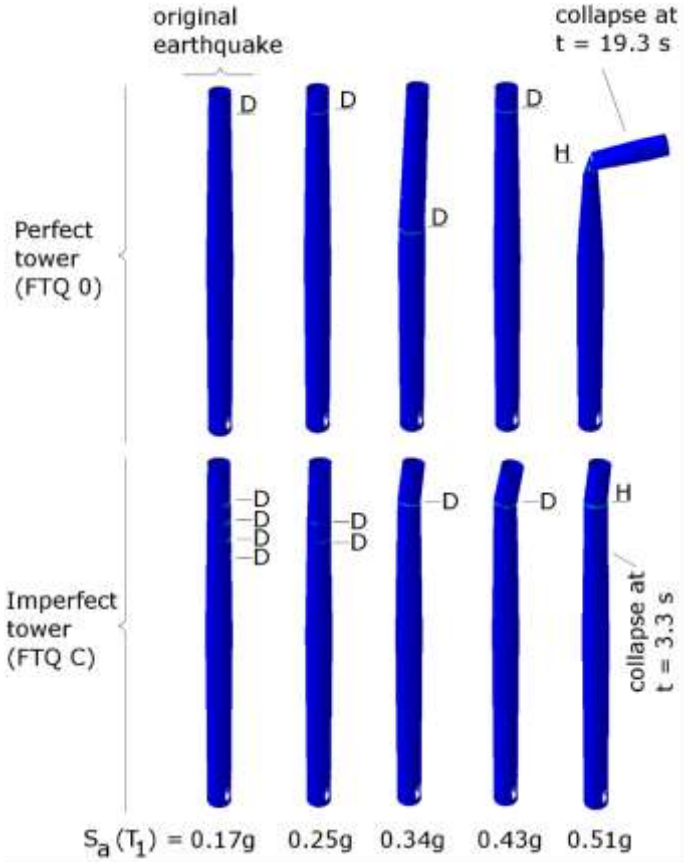

Figure 6. Deformed configuration of the tower at the end of the analysis in the near-field earthquake for different intensities. 'D' means damage section and 'H' is a full hinge. RSN 8157.

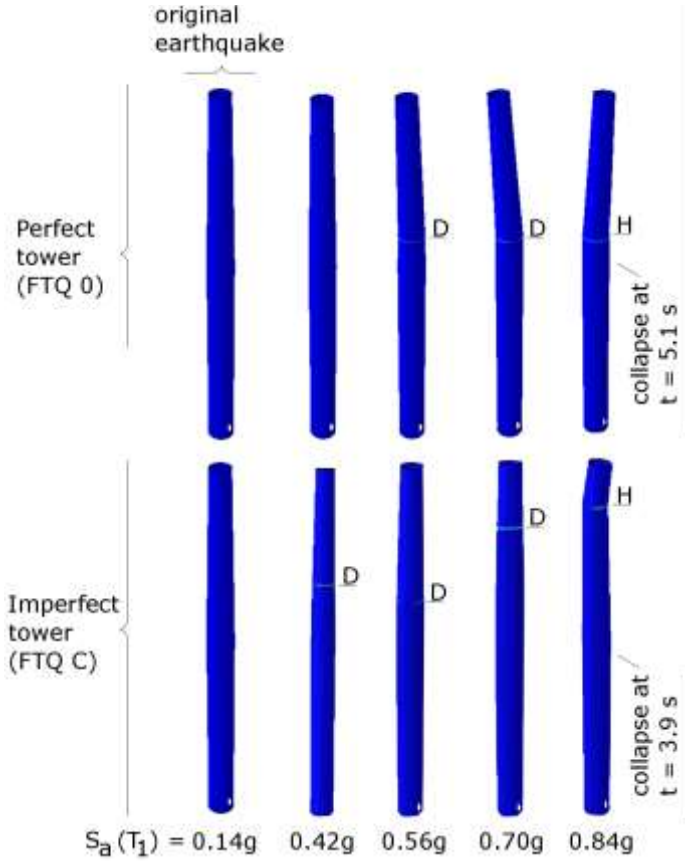

Figure 7. Deformed configuration of the tower at the end of the analysis in the far-field earthquake for different intensities. 'D' means damage section and 'H' is a full hinge. RSN 451.

6 CONCLUSIONS

This study focused on the elastic and the inelastic seismic responses of a conventional steel-tower wind turbine subject to earthquakes with different rupture distances (R_{epi}).

The elastic analysis considered a significant number of recorded earthquakes (2,660 in total). It was observed that the spectral acceleration at the fundamental mode of the tower ($S_a(T_1)$) is an efficient intensity measure to describe the demand of displacements during the earthquake. The results indicate that the earthquakes with epicentral distances between 20 and 120 km have a slightly larger influence in terms of the peak displacements but generally speaking if the earthquakes are scaled to the same $S_a(T_1)$ the elastic tower displacements are almost the same, regardless of the shape of their acceleration spectra. However, the bending moment along the tower seems to be more influenced by higher-order vibration modes and the $S_a(T_1)$ loses efficiency to describe this response measure.

Two earthquakes are selected from the previous data set to conduct the nonlinear dynamic analysis. The records have different rupture distances but they are similar in terms of the type of ground where they were recorded, their moment magnitude, their significant duration (approximately 30 s) and their original $S_a(T_1)$. One of this records is near-field (R_{epi} = 1.11 km) and the other is far-field (R_{epi} = 30.05 km). A nonlinear seismic analysis was conducted on a detailed model of the tower that includes realistic weld imperfections represented with axisymmetric depressions at the connections between the steel segments of the structure. Series of incremental dynamic analysis were conducted with and without imperfections. It was observed that the weld depressions can have a significant effect in the seismic response of the structure and potentially reduce significantly the intensity threshold of the earthquakes that can damage or even destroy the wind turbine, and it can also accelerate the development of a full plastic hinge at a weld depression that triggers a rapid failure. Therefore, it is recommended to model the imperfections in the seismic analysis of these structures and to explore their effect with further research. In addition, comparing the two earthquakes it is observed that the position of the plastic hinge when the tower collapses occurs at higher regions in the near-field record. These regions have less dissipation capacity and the seismic response induced by the near-field earthquake represents a higher risk. This is attributed to the larger contribution of high-order modes in the excitation of the regions of the tower closer to its top.

The results obtained are consistent with previous works, which observed that ground motions corresponding to rocky grounds tend to lift the position of the plastic hinge in the tower and to reduce its capacity due to the lower dominant periods in this records (Zhao *et al*., 2019). The results of this work suggests that distance between the wind turbine and the epicenter, and not only $S_a(T_1)$, is important for the seismic design of these structures. Further studies with a larger number of records considered in the nonlinear dynamic analysis need to be conducted to fully explore the influence of the spectral shape on the seismic behaviour of wind turbine towers.

REFERENCES

ABAQUS. 2017. ABAQUS Version 6.17, Commercial Finite Element Software. Dassault Systèmes, Simulia Corporation, Providence: RI, USA.

Ancheta TD, Darragh RB, Stewart JP, Seyhan E, Silva WJ, Chiou BSJ, Wooddell KE, Graves RW, Kottke AR, Boore DM, Kishida T & Donahue JL. 2013. PEER-NGA West2 database. Pacific Earthquake Eng. Research Centre, Report PEER 2013/03, May 2013.

Dai K, Bergot A, Liang C, Xiang WN & Huang WN. 2015. Environmental issues associated with wind energy – a review. *Renewable Energy*, 75: 911-921.

Dai K, Sheng C, Zhao Z, Yi Z, Camara A & Bitsuamlak, G. 2017. Nonlinear response history analysis and collapse mode study of a wind turbine tower subjected to tropical cyclonic winds. *Wind and Structures*, 25(1): 79-100.

Katsanos EI, Thons S & Georgakis CT. 2016. Wind turbines and seismic hazard: a state-of-the-art review. *Wind Energy*. 19(11): 2113-2133.

Nuta E, Christopoulos C & Packer JA. 2011. Methodology for seismic risk assessment for tubular steel wind turbine towers: application to Canadian seismic environment. *Canadian Journal of Civil Engineering*. 38: 293–304.

Sadowski AJ, Camara A, Málaga-Chuquitaype C & Dai K. 2017. Seismic analysis of a tall metal wind turbine support tower with realistic geometric imperfections. *Earthquake Engineering and Structural Dynamics*. 46: 201-219.

Zhao Z, Dai K, Camara A, Bitsuamlak & Sheng C. 2019. Wind turbine tower failure modes under seismic and wind loads. *Journal of Performance of Constructed Facilities (ASCE)*. 33(2).